Phys. Proc. Ultra-Peripheral Collisions **2**, 010 (2025) 1-5

Invariant Mass Dependence of the Entanglement-Enabled Spin Interference effect at STAR

S. Corey[a] (for the STAR Collaboration)
191 W Woodruff Ave, Columbus, Ohio, 43210, United States of America

In 2023, the STAR collaboration reported a measurement of an azimuthal angular anisotropy in pion pairs produced in ultra-peripheral collisions. This anisotropy is attributed to double-slit-like interference between $\rho^0(770)$ meson production channels where opposite nuclei act as the photon emitter. However, the anisotropy has not been measured at pair invariant mass values far from the $\rho^0(770)$ mass. We report the first measurement of the mass dependence of this angular anisotropy, which reveals the presence of contributions from interference between the ρ^0 and the continuum. Additionally, by cross-referencing the strength of the anisotropy with the two-pion invariant mass cross section, we obtain additional information on resonant states heavier than the $\rho^0(770)$, such as the $\rho(1700)$.

DOI: https://doi.org/10.17161/rtz8f070
Keywords: photonuclear interactions, hadron spectroscopy, azimuthal anisotropy

1 Introduction

In ultra-peripheral heavy-ion collisions (UPCs), linearly polarized photons from the strongly Lorentz-contracted electromagnetic fields of the nuclei mediate interactions between the two nuclei. The two-pion final state, produced dominantly through the photonuclear process, where one nucleus emits a photon which then fluctuates into a quark-anti-quark pair and interacts with the other nucleus through a Pomeron, has been the target of UPC physics for decades [2 3].

Photonuclear production of the ρ^0 meson can occur through two distinct channels in which different nuclei act as the photon emitter (see Fig. 1). Quantum interference similar to that of the double-slit experiment between these two channels leads to a unique azimuthal angular anisotropy in the final state, consisting of two pions from the ρ^0 decay [1]. The total spin carried by each of the interfering processes, originating from the linearly polarized photons, results in a $\cos(2\Delta\phi)$ angular anisotropy in the final state, where $\Delta\phi = \angle(p_T^{\pi^+} + p_T^{\pi^-}, p_T^{\pi^+} - p_T^{\pi^-})$ (see Fig. 2). Because the ρ^0 meson decays at a length scale smaller than the separation between nuclei, the wavefunction overlap occurs at the level of the entangled pion pairs.

Importantly, the interfering photonuclear production channels are not identical, classically forbidding interference between them. The recently developed framework of Cotler-Wilczek interference provides an explanation [4]. In Cotler-Wilczek processes, orthogonal eigenstates are made to interfere by first applying a unitary transformation that mixes and entangles the states, then filtering for only one of the states before measuring. The interference producing the $\cos(2\Delta\phi)$ anisotropy is an example of an *inverse* Cotler-Wilczek process, where the intermediate ρ^0 state, which acts as a filter, comes before the decay that provides the entangled pion pair [5].

In this work, we report the measurement of the mass dependence of the $\cos(2\Delta\phi)$ modulation strength in exclusively produced pion pairs from UPCs at the STAR experiment. If only pions originating from the decay of a ρ^0 are considered, there is no reason to expect change in modulation strength as a function of pair invariant mass. However, other production channels such as continuum or other resonant states contribute to the total cross section. The interference between these channels and the ρ^0 may have different interference strengths, leading to mass dependence of the $\cos(2\Delta\phi)$ modulation strength.

[a]Samuel Corey, email: corey.90@osu.edu

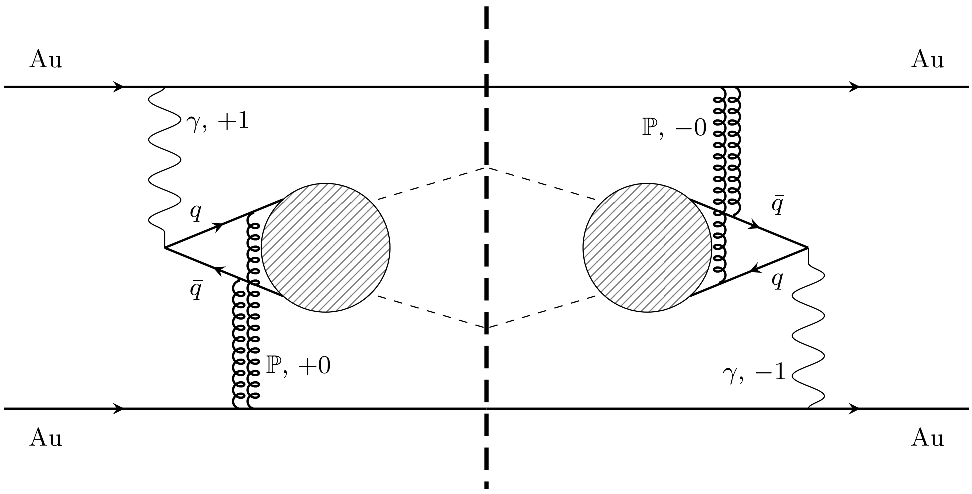

Figure 1: Feynman diagram illustrating the double-slit-like interference effect between photonuclear channels where opposite nuclei act as the photon emitter. Numbers indicate the angular momentum quantum numbers contributed by each incident particle, and the narrow dashed lines represent the pion propagators. The thick dashed line represents interference between the left- and right-hand processes.

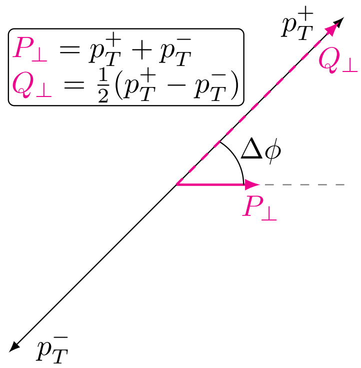

Figure 2: $\Delta\phi$ is the angle in the transverse plane between the sum and the difference between the momenta of the two pions. The interference between two processes produces an anisotropy in the $\Delta\phi$ distribution.

Additionally, presence of two-pion production originating from two-photon fusion, which has not yet been observed in nuclear collisions, would lead to pion pairs that do not contribute to the $\cos(2\Delta\phi)$ modulation, leading to a decrease in the modulation strength at mass values where this production mechanism has the largest contribution. As such, the measurement of the mass dependence of the $\cos(2\Delta\phi)$ provides new insight into the interference effect itself and the nature of higher-mass resonances produced in UPCs.

2 Dataset and Two-Pion Event Selection

The pion pairs used in this analysis were produced in Au+Au collisions with $\sqrt{s_{NN}} = 200\,\mathrm{GeV}$ at RHIC, and measured using the STAR experiment. UPC events are selected by requiring low multiplicity of hits in the Time Of Flight (TOF) detector, coincidence of neutrons detected in both Zero Degree Calorimeters (ZDCs), and no activity in the Beam-Beam Counters (BBCs). This minimizes the contamination from peripheral hadronic collisions. Information from the Time Projection Chamber (TPC), which, along with the TOF, covers a pseudorapidity range of approximately −1 to 1, is used to identify events with exactly two pions with opposite sign and no other particles present. The pion Lorentz vectors are then reconstructed from the TPC tracks.

3 Azimuthal Angular Anisotropy

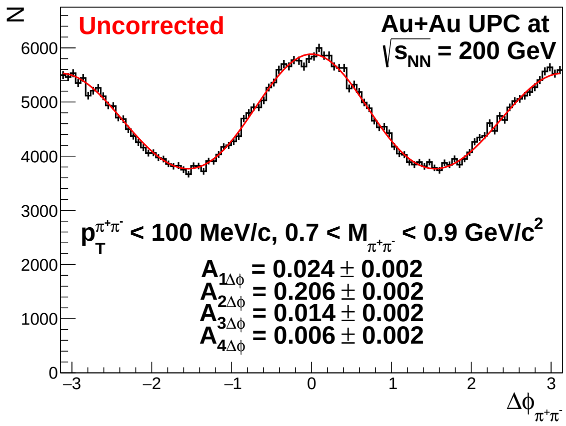

Figure 3: Uncorrected $\Delta\phi$ distribution at low p_T in the mass region surrounding $\rho^0(770)$. The distribution is fitted with a Fourier series (Eq. (1)) to extract the harmonics $A_{n\Delta\phi}$ which quantify the interference signal strength.

The uncorrected $\Delta\phi$ distribution at low pair transverse momentum in the mass range of the $\rho^0(770)$ is shown in Fig. 3. Due to STAR's 2π acceptance in azimuth and pion detection momentum threshold, the acceptance and efficiency correction in this kinematic range is negligible. The distribution is fit with a Fourier series of cosines,

$$C[1 + A_{1\Delta\phi}\cos(\Delta\phi) + A_{2\Delta\phi}\cos(2\Delta\phi) + A_{3\Delta\phi}\cos(3\Delta\phi) + A_{4\Delta\phi}\cos(4\Delta\phi)], \tag{1}$$

as shown in Eq. (1), where C is an overall normalization constant and A_n represent the strengths of the $\cos(n\Delta\phi)$ modulation.

The extracted parameter $A_{2\Delta\phi}$ reproduces the previously measured double-slit-like interference in the mass range surrounding the $\rho^0(770)$ meson. Differential measurement of the modulation strengths as a function of pair invariant mass requires proper handling of unique acceptance effects in $\Delta\phi$. These effects are strongest in cases where one pion is typically near or below the transverse momentum threshold for detection, around 200 MeV/c. To do this, the measured $\Delta\phi$ distribution, $\gamma(\Delta\phi)$, is taken to be the product of the true signal $\alpha(\Delta\phi)$ and the acceptance effect $\omega(\Delta\phi)$. The Fourier coefficients γ_n are defined in the following way:

$$\gamma_n = 2\frac{\int_{-\pi}^{\pi}\alpha(\Delta\phi)\omega(\Delta\phi)\cos(n\Delta\phi)d\Delta\phi}{\int_{-\pi}^{\pi}\alpha(\Delta\phi)\omega(\Delta\phi)d\Delta\phi}. \tag{2}$$

The integral definition in Eq. (2) is then solved by expanding $\alpha(\Delta\phi)$ and $\omega(\Delta\phi)$ as Fourier series. For simplicity and computational stability, the correction for a particular Fourier coefficient n is carried out assuming that all terms in the Fourier expansions of $\alpha(\Delta\phi)$ and $\omega(\Delta\phi)$ are equal to zero except for the n^{th} term. Under this assumption, the integral can be easily computed and inverted to express the true coefficient α_n as a function of γ_n and ω_n,

$$\alpha_n = \frac{-2(\gamma_n - \omega_n)}{\gamma_n\omega_n - 2}. \tag{3}$$

Equation (3) is applied as a correction to the data.

The distortion weight distribution $\omega(\Delta\phi)$ is obtained with a simple two-body decay toy model. The pion distributions from this toy model are then reweighted to match the π^+ and π^- p_T and η distributions from the data, precisely reproducing the distortion in the $\Delta\phi$ distribution. Applying Eq. (3) separately in each p_T and $M_{\pi\pi}$ bin allows for a model-independent and data-driven correction methodology. Projecting these three-dimensional representations into two dimensions produces the results shown in Fig. 4.

Figure 4 shows the fully corrected $cos(2\Delta\phi)$ signal strength as a function of pair invariant mass for the first time. Data below 900 MeV/c^2 lie in the mass range previously studied by STAR [1]. Above this value, the data follows a decreasing trend, until approximately 1600 MeV/c^2, where the modulation strength

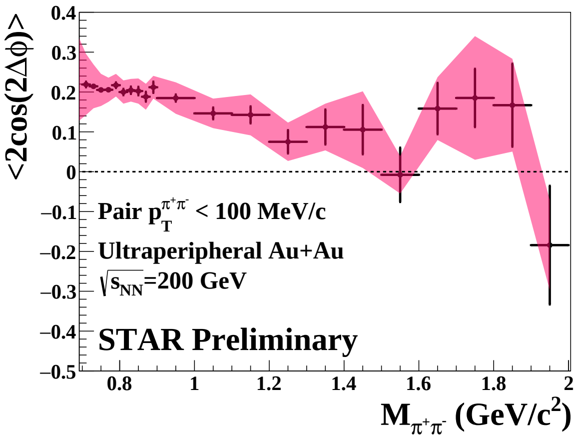

Figure 4: The modulation strength $\langle 2\cos(2\Delta\phi)\rangle$ as a function of pair invariant mass. Data and statistical uncertainties are represented by the black points, and systematic uncertainties by the shaded region.

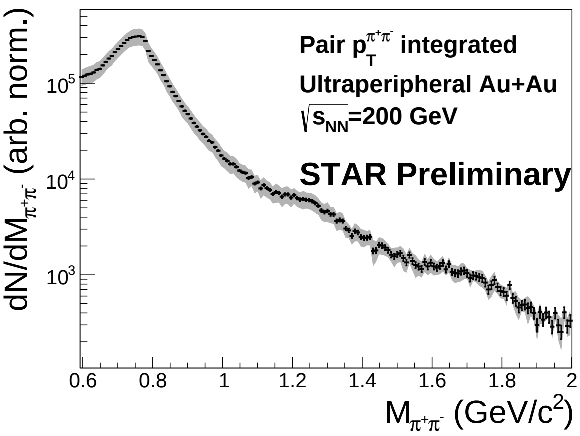

Figure 5: Invariant mass spectrum of exclusively produced pion pairs, corrected for efficiency and acceptance.

returns to near its low-mass value. To further understand these features, the interference measurement must be compared to the invariant mass spectrum.

In the invariant mass spectrum (Fig. 5), the well-known features around the ρ^0 peak at $770\,\mathrm{MeV}/c^2$ are present. The apparent shift of the mass at the maximum yield appears due to the interference between continuum photonuclear production of $\pi^+\pi^-$ pairs, the so-called Drell-Söding process. Small contribution from the ω meson with a mass of $782\,\mathrm{MeV}/c^2$ appears as a small "shoulder" in the distribution [3]. Additionally, there are two new wide resonances near $1300\,\mathrm{MeV}/c^2$ and $1700\,\mathrm{MeV}/c^2$ not described by previous STAR analyses.

Unlike the lower mass states, which are relatively unambiguous, these higher mass resonances cannot be identified by their mass alone due to the high density of states that could explain these features [6]. Some of these states, such as the $J = 2$ $f_2(1270)$ and $J = 1$ $\rho(1450)$ for the structure near $1300\,\mathrm{MeV}/c^2$ and the $J = 1$ $\rho(1700)$ and $J = 3$ $\rho_3(1690)$ near $1700\,\mathrm{MeV}/c^2$, can only be comfortably distinguished, at the precision level of modern experiments, by identifying their spin. The interference signal strength shown in Fig. 4 allows access to this information.

The decreasing trend in Fig. 4 below $1600\,\mathrm{MeV}/c^2$ indicates the presence of interference effects other than the double-slit-like interference in ρ^0 production. The interference between ρ^0 and the Drell-Söding process is destructive in this mass range, leading to the apparent rightward shift in the mass of the main peak. This negative contribution to the overall cross section corresponds to a negative contribution to the $\cos(2\Delta\phi)$ modulation strength. Additionally, the decreasing trend is consistent with increasing contribution from photon-photon fusion, which reaches its maximum at $1270\,\mathrm{MeV}/c^2$ due to the $f_2(1270)$ meson [7]. Due to the presence of the interference between ρ^0 and the Drell-Söding process, this measurement alone does not provide definitive evidence of pion pairs produced in photon-photon fusion in UPCs. Lack of a significant feature at $1450\,\mathrm{MeV}/c^2$, however, disfavors the description of the apparent resonance near $1300\,\mathrm{MeV}/c^2$ in Fig. 5 as solely belonging to the $\rho(1450)$ meson.

Additionally, the apparent feature in Fig. 4 at $1750\,\mathrm{MeV}/c^2$ is consistent with both the $\rho(1700)$ and $\rho_3(1690)$ mesons. However, the Tensor (spin-2) Pomeron exchange required to produce a spin-3 meson such as $\rho_3(1690)$ is rarer than the spin-0 Pomeron exchange and contributes primarily above the pair transverse momentum range of this analysis [8]. As a result, this contribution is most likely due to the spin-1 $\rho(1700)$ meson and its interference with the $\rho^0(770)$ tail and the Drell-Söding continuum, as well as the double-slit like interference in $\rho(1700)$ production.

4 Conclusion

We report the invariant mass dependence of the $\cos(2\Delta\phi)$ modulation previously discovered by the STAR collaboration [1]. This effect has previously been attributed to double-slit like interference between photonuclear ρ^0 production with opposite nuclei acting as the photon emitter. However, the invariant mass dependence of $\langle 2\cos(2\Delta\phi)\rangle$ indicates contribution from other interference terms previously explored in the context of the invariant mass spectrum of UPC pion pairs [3]. This result is qualitatively consistent with expectations due to a combination of these interference terms and the presence of pion pairs produced via photon-photon fusion.

Comparison of $\langle 2\cos(2\Delta\phi)\rangle$ with the features of the invariant mass spectrum itself illuminates the nature of the higher-mass resonances seen in Fig. 5. The feature in the spectrum at $1300\,\mathrm{MeV}/c^2$, typically interpreted as the $J = 1$ $\rho(1450)$ is not accompanied by any significant feature in the invariant mass dependence of $\langle 2\cos(2\Delta\phi)\rangle$, disfavoring the description of the feature as a $J = 1$ state. On the other hand, there is a significant increase in the modulation strength near $1750\,\mathrm{MeV}/c^2$, suggesting that the resonance seen in this location on the invariant mass spectrum is indeed the $\rho(1700)$.

Acknowledgments

This work is supported in part by the Office of Nuclear Physics within the U.S. DOE Office of Science.

References

1. The STAR Collaboration, Sci. Adv. **9**, abq3903 (2023) doi:10.1126/sciadv.abq3903
2. The STAR Collaboration, Phys. Rev. Lett. **89**, 272302 (2002) doi:10.1103/PhysRevLett.89.272302
3. The STAR Collaboration, Phys. Rev. C **96**, 054904 (2017) doi:10.1103/PhysRevC.96.054904
4. J. Cotler, F. Wilczek, V. Borish arXiv:1607.05719 doi:10.48550/arXiv.1607.05719
5. J. D. Brandenburg, H. Duan, Z. Tu, R. Venugopalan, Z. Xu Phys. Rev. Research **7**, 013131 (2025) doi:10.1103/PhysRevResearch.7.013131
6. S. Navas et al. (Particle Data Group), Phys. Rev. D **110**, 030001 (2024) doi:10.1103/PhysRevD.110.030001
7. I. Danilkin, C. F. Redmer, and M. Vanderhaeghen, Prog. Part. Nucl. Phys. **107**, 20 (2019) doi:10.1016/j.ppnp.2019.05.002
8. Y. Hagiwara, C. Zhang, J. Zhou, and Y. Zhou Phys. Rev. D **104**, 094021 doi:10.1103/PhysRevD.104.094021